ELSEVIER

Journal of Chromatography B, 715 (1998) 229–244

JOURNAL OF CHROMATOGRAPHY B

Review

Retention data from affinity high-performance liquid chromatography in view of chemometrics

Roman Kaliszan

Medical University of Gdańsk, Department of Biopharmaceutics and Pharmacodynamics, Gen. J. Hallera 107, Pl-80-416 Gdańsk, Poland

Abstract

A combination of affinity chromatography and chemometrics is demonstrated to provide information on drug analytes and on biomacromolecules forming stationary phases, which is of relevance to molecular pharmacology and to rational drug design. The approach can also be applied to elucidate the molecular mechanism of enantioseparation on natural biopolymer stationary phases. Affinity high-performance liquid chromatographic data, which were determined on silica-based human serum albumin, α_1-acid glycoprotein, keratin, collagen, melanin and amylose tris(3,5-dimethylphenylcarbamate) stationary phases, are discussed. Quantitative structure–retention relationships (QSRRs) derived for test series of drug analytes are interpreted in terms of structural requirements of specific binding sites on biomacromolecules. A means to quantify the differences in drug–biomacromolecule binding among the members of analyte families is demonstrated based on hydrophobicity and structural descriptors from molecular modeling. Chemometric processing of appropriately designed sets of affinity chromatographic data may increase the speed and efficiency of a search for new drugs, providing at the same time a chance to reduce the number of in vivo screenings. It can also be of help in rational selection of chiral columns for specific analytical separations.

Keywords: Chemometrics; Retention data; Reviews; Human serum albumin; α_1-Acid glycoprotein; Keratin; Collagen; Melanin; Amylose tris(3,5-dimethylphenylcarbamate)

Contents

0378-4347/98/$19.00
PII: S0378-4347(98)00175-3

1. Introduction

It is considered that the same basic intermolecular interactions determine the behavior of chemical compounds in both biological and chromatographic environments [1]. Modern techniques and procedures of high-performance liquid chromatography (HPLC) and capillary electrophoresis (CE) allow for inclusion of various biomacromolecules as active components of chromatographic systems. Proteins immobilized (either physically or chemically) on a solid matrix (usually microparticulate silica) form stationary phases for affinity HPLC.

The high level of complexity of biological systems limits the rational design of individual chromatographic systems that would directly mimic them. Conversely, chromatography is a unique method that can readily yield a great amount of diversified, precise and reproducible data for large series of chemical compounds. In a chromatographic process, all of the experimental conditions can be kept constant and the analyte structure becomes the single independent variable in the physicochemical system. It can be presumed that chemometric processing of appropriately designed and selected sets of chromatographic data can reveal systematic information regarding both the analytes (usually drugs and other xenobiotics) and the affinity stationary phases studied [2].

Protein stationary phases (PSPs) for HPLC were introduced in the early 1980s [3–5]. PSPs, such as bovine serum albumin (BSA) [6], α_1-acid glycoprotein (AGP) [7] and human serum albumin (HSA) [8], found wider analytical applications for enantiospecific determinations of chiral drugs. Also, for enantioselective separations, affinity HPLC supports containing ovomucoid [9], flavoprotein [10], avidin [11] and pepsin [12] were developed.

It has long been realized that separation techniques, such as liquid chromatography and subsequently CE, can be used to conveniently quantify drug–protein binding. Numerous papers were published on this subject, which has also been discussed critically in reviews by Sebille et al. [13], Soltes and Sebille [14], Oravcová et al. [15] and Gao et al. [16]. After the latter review, an exhaustive review by Hage and Tweed [17] appeared in this journal reporting new methodological aspects of the HPLC and CE techniques for studies of drug–protein binding. This will not be reviewed here.

There are numerous reports regarding the application of affinity CE and HPLC to solve analytical problems and to evaluate the strength of drug–protein interactions. However, the combination of affinity chromatography and chemometrics is a research strategy that was very recently introduced and developed [18,19]. Such a combined approach, aimed at providing information of relevance to molecular pharmacology and for drug design, is discussed in this review.

2. Human serum albumin column

Human serum albumin is a serum protein that binds mainly acidic and neutral drugs. Because only the free (unbound) fraction of a drug in blood can undergo the processes of distribution to tissues (the actual sites of pharmacological actions), it is important to determine drug–protein interactions. Affinity HPLC on immobilized protein stationary phases can be a convenient tool for studying such interactions [20,21].

A series of benzodiazepine derivatives (Fig. 1) was subjected to HPLC analysis [22]. The set of 22 compounds included nine achiral solutes, nine racemic mixtures and four single enantiomers. The compounds were chromatographed on a HSA–PSP. The mobile phase was sodium dihydrogen phosphate–disodium hydrogen phosphate buffer, pH 6.90, modified with 5% (v/v) propanol.

In the analysis [23] of quantitative structure–enantiospecific retention relationships (QSERRs) for chiral solutes, the logarithms of retention factors corresponding to both the first peak, log k_P, and the second peak, log k_M, were considered. Retention parameters of the achiral agents, log k_{AC}, were analyzed independently. The structure of the compounds were characterized by means of the following parameters (Fig. 2): C_3, quantum chemically calculated electron excess charge on carbon C_3; P_{SM}, the excess charge difference between the hydrogen atom at C_3 and the most negatively charged atom in the other substituent at C_3, multiplied by the distance (in Å) between these two atoms; W, the width of the molecule along the phenyl substituent; f_{X+Y}, the sum

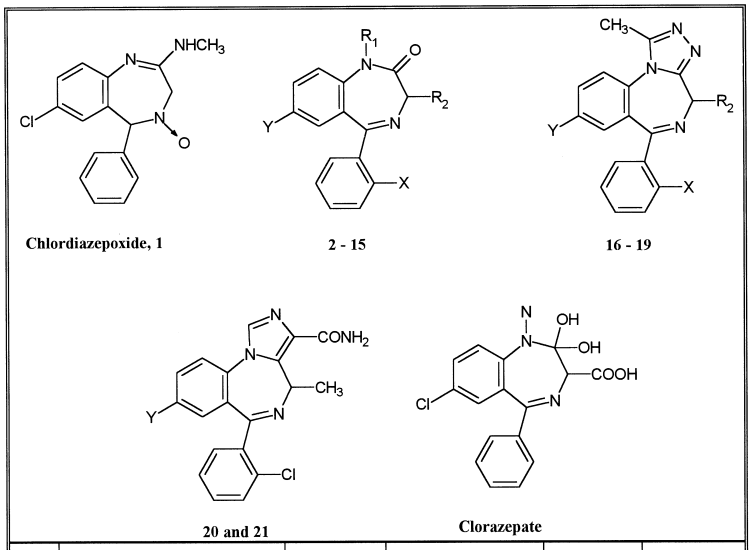

No.	Compound	R_1	R_2	X	Y
1	Chlordiazepoxide	See above			
2	(R, S)-Oxazepam H	H	$OCO(CH_2)_2COO$	H	Cl
3	Nitrazepam	H	H	H	NO_2
4	Flunitrazepam	CH_3	H	F	NO_2
5	Clonazepam	H	H	Cl	NO_2
6	Delorazepam	H	H	Cl	Cl
7	Desmethyldiazepam	H	H	H	Cl
8	Diazepam	CH_3	H	H	Cl
9	(R, S)-Lormetazepam	CH_3	OH	Cl	Cl
10	(R, S)-Lorazepam	H	OH	Cl	Cl
11	(R, S)-Oxazepam	H	OH	H	Cl
12	(R, S)-Temazepam	CH_3	OH	H	Cl
13	(S)-Ro 14-8935/000	CH_3	CH_3	Cl	NH_2
14	(S)-Ro 23-0983/001	H	CH_3	Cl	F
15	(R, S)-Ro 11-3128/002	H	CH_3	Cl	NO_2
16	(R, S)-Alprazolam, 4-OH		OH	H	Cl
17	Alprazolam		H	H	Cl
18	Triazolam		H	Cl	Cl
19	(S)-Ro 11-5073/000		CH_3	F	Cl
20	(S)-Ro 23-1117/000				F
21	(R, S)-Ro 23-3880/000				Cl
22	Clorazepate	See above			

Fig. 1. Benzodiazepine analytes chromatographed on a human serum albumin (HSA) HPLC column.

of the hydrophobic constants of the substituent at position 7 in the fused benzene ring plus that of the substituent at position 2′ of the phenyl substituent. Numerical data are assembled in Table 1.

At first, a highly significant regression equation was obtained relating retention of the second-eluting enantiomer, which is assumed to bind in the M conformation, log k_M, and retention of the first-eluting enantiomer, which is assumed to bind in the P conformation, log k_P:

$$\log k_M = 1.097(\pm 0.162) \log k_P + 0.547(\pm 0.067) P_{SM} - 0.149$$

$$n = 9; R = 0.980; F = 61; p \leq 3 \times 10^{-4} \quad (1)$$

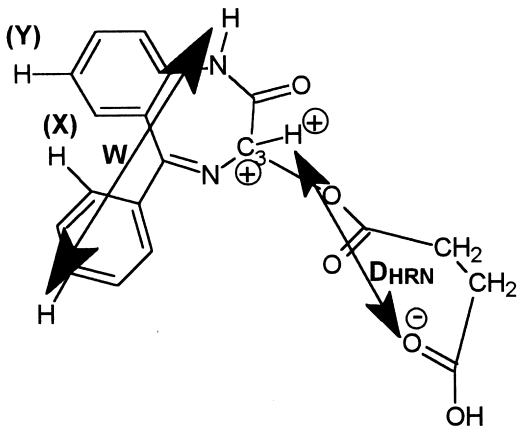

Fig. 2. Structural descriptors of benzodiazepines used in quantitative structure–enantiospecific retention relationship (QSERR) equations. See text for explanation.

where n is the number of analytes considered in deriving the regression equation, R is the multiple correlation coefficient, F is the value of the F-test of significance and p is the significance level of the equation. Numbers in parentheses are standard deviations of regression coefficients.

The retention of the first eluted enantiomer was described by the following equation:

$$\log k_P = 0.183(\pm 0.079)\ f_{X+Y} - 0.278(\pm 0.055)W + 2.479 \quad (2)$$

$$n = 13;\ R = 0.845;\ F = 12.5;\ p \leq 2 \times 10^{-3}$$

Eq. (2) suggests that retention (or binding) takes place at a site that contains a hydrophobic pocket and that access to that site is sterically restricted.

Table 1
Logarithms of chromatographic retention factors determined on a human serum albumin HPLC column and structural parameters from molecular modeling of a series of benzodiazepine derivatives [23]

No.[a]	log k_P [b]	log k_M [c]	log k_{AC} [d]	P_{SM} [e]	f_{X+Y} [f]	C_3^g	W[h]
1			0.8645	0.0849	1.05	0.1035	9.30
2	0.8512	1.8938		1.8635	1.05	0.2785	8.74
3			0.6243	0.0703	0.06	0.0960	8.54
4			0.4857	0.0609	0.20	0.0882	9.63
5			0.7679	0.0680	0.77	0.0966	8.67
6			1.0614	0.0635	1.76	0.0977	8.69
7			1.0969	0.0634	1.05	0.0979	8.59
8			1.1216	0.0578	1.05	0.0933	9.56
9	0.7672	0.9745		0.6120	1.76	0.2388	9.76
10	0.8068	0.9360		0.5953	1.76	0.2425	8.71
11	0.6561	1.0261		0.7049	1.05	0.2451	8.60
12	0.5224	1.1793		0.6113	1.05	0.2353	9.49
13	0.3892			0.0675	−0.18	0.0549	10.0
14	0.6628			0.0600	1.19	0.0624	8.64
15	0.7193	0.7193		0.0633	0.77	0.0651	8.70
16	0.2648	0.4533		0.5862	1.05	0.3169	10.5
17			0.4200	0.0784	1.05	0.1722	10.3
18			0.6243	0.0730	1.76	0.1725	10.3
19	0.3838			0.0484	1.19	0.1379	10.2
20	0.7404			0.0320	1.19	0.1309	9.20
21	1.0523	1.1156		0.0441	1.76	0.1184	9.22
22	0.9715	1.3992		1.0745	1.05	0.0916	8.14

[a] Compounds are numbered as in Fig. 1.
[b] Retention parameter of the first-eluting enantiomer.
[c] Retention parameter of the second-eluting enantiomer.
[d] Retention parameter of achiral solutes.
[e] Submolecular polarity parameter (see Fig. 2).
[f] Sum of hydrophobic constants of substituents X and Y.
[g] Electron excess charge on carbon C_3 of the diazepine system.
[h] Molecular width (in Å).

The retention of the second-eluting enantiomer of benzodiazepines is described by the following equation:

$$\log k_M = 0.835(\pm 0.154)\, P_{SM} + 0.364(\pm 0.199)\, f_{X+Y} - 2.690(\pm 0.932)\, C_3 + 0.556 \quad (3)$$

$n = 8; R = 0.938; F = 10; p \leq 0.03$

Eq. (3) indicates that binding of conformers *M* of benzodiazepines occurs at a site that contains both a hydrophobic pocket and a positively charged area. The cationic region of the binding site produces an attractive interaction with the submolecular dipole quantified by P_{SM} and a repulsive interaction with the excess positive charge at C_3.

The retention of achiral benzodiazepines was described as:

$$\log k_{AC} = 0.374(\pm 0.096)\, f_{X+Y} - 7.068(\pm 1.663)\, C_3 + 1.221 \quad (4)$$

$n = 9; R = 0.889; F = 11; p \leq 0.01$

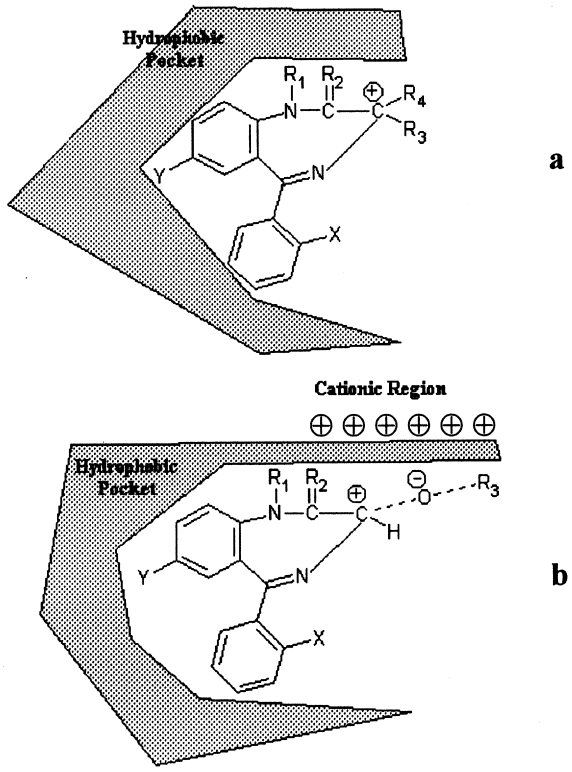

Fig. 3. Two postulated modes of benzodiazepine binding to human serum albumin. See text for discussion.

Since for achiral benzodiazepines, the parameter P_{SM} is zero, Eq. (4) indicates that these compounds predominantly bind in the *M* conformation, as reported in the literature [24].

Based on Eqs. (1)–(4), a model was proposed [23] for the structural requirements for two postulated modes of benzodiazepine binding to HSA (Fig. 3). According to Eq. (2), benzodiazepines appear to bind within hydrophobic cavities, and substituents at N_1, C_2 and C_5 would then provide spatial orientation of the analyte molecules within this cavity. Steric limitations suggest that the hydrophobic cavity has definite boundaries. The steric features at the stereogenic center, carbon C_3, appear to play no role in this binding mode (Fig. 3a).

The binding mode of the second-eluting enantiomer, as described by Eq. (3), involves hydrophobic and electrostatic interactions. Thus, in addition to a hydrophobic cavity, there must be a cationic region in close proximity (Fig. 3b). For the benzodiazepines in the M conformation, the electrostatic repulsion between the excess positive charge on carbon C_3 and the cationic site on the protein surface appears to be more than offset by the attraction of a negatively charged atom within the substituent at C_3 and the same area. In the case of the less retained enantiomer, the electrostatic repulsion between carbon C_3 and the cationic area, on the one hand, and the steric hindrance due to the P conformation, on the other, may prohibit binding at this site.

The structure of the HSA–benzodiazepine binding site that has emerged from the QSERR analysis appears to be consistent with the structure derived from X-ray crystallographic studies.

There is one more short QSRR study concerning retention on the HSA column described in the literature [25]. According to that study, binding of six indolocarbazole antiviral agents to HSA increases with their increasing lipophilicity and acidity.

3. α_1-Acid glycoprotein column

α_1-Acid glycoprotein (AGP) is a serum protein that binds mainly basic drugs [26]. The prevalent view is that AGP has only one common drug binding site, which binds drugs through hydrophobic and electrostatic interactions [27,28]. However, neither log *P* [27,29] nor pK_a [30] could account for binding differences within small sets of tested drugs.

Retention factors, log k_{AGP}, were determined for 52 basic drugs of diverse chemical structures and pharmacological activities on an AGP–PSP [31–33]. The column was packed with human AGP that was chemically bound to 5 μm silica particles. The mobile phase was 2-propanol–phosphate buffer (0.1 *M*, pH 6.5) 5:95 (v/v). The eluent flow-rate was 0.5 ml/min and UV absorbance detection was at 215 nm. The log k_{IAM} parameters for the set of agents studied were also determined using an immobilized artificial membrane (IAM) column, which was introduced [34,35] to mimic the lipophilic properties of biological membranes. The IAM columns were demonstrated [36,37] to produce biologically relevant measures of hydrophobicity of drug analytes.

Molecular modeling was employed to determine the solutes' structural parameters, which were important for describing their interactions with AGP. The following parameters were used: Electron excess charge on an aliphatic nitrogen atom, N_{ch}, and the surface area, S_T, of a triangle having one vertex on the aliphatic nitrogen and the two remaining vertices on the extremely positioned atoms in the drug molecule (Fig. 4) [32]. Structural parameters from molecular modeling and retention data determined on the AGP and IAM columns are given in Table 2.

The QSRR equation relating retention on chemically immobilized AGP to a hydrophobicity measure, log k_{IAM}, electron excess charge on aliphatic nitrogen, N_{ch}, and a size parameter, S_T, of drugs has the form:

$$\log k_{AGP} = 0.6577(\pm 0.0402) \log k_{IAM} + 3.342(\pm 0.841)N_{ch} - 0.0081(\pm 0.0030)S_T + 1.688(\pm 0.245) \quad (5)$$

$n = 49$; $R = 0.929$; $s = 0.163$; $F = 92$; $p \leq 10^{-5}$

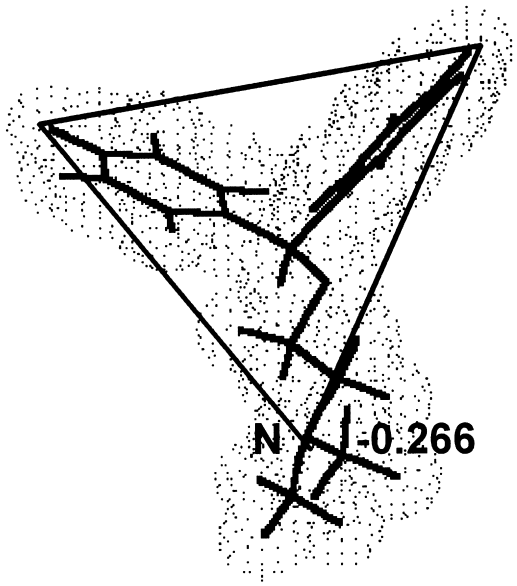

Fig. 4. Structural descriptors of basic drugs chromatographed on a human α_1-acid glycoprotein (AGP) column used in quantitative structure–retention relationships (QSRR) studies. See text for explanation.

Of the 52 drugs studied, three (triprolidine, cimetidine and bopindolol) did not fit Eq. (5). The reason may be the uncertainty in identifying the atom equivalent to the aliphatic nitrogen with regard to electrostatic interactions.

Eq. (5) may be useful in drug design as a first approximation of relative binding of an agent to AGP, without the need to perform biochemical experiments. It can also indicate relative differences in AGP binding among individual drugs and help to predict the probability of pharmacokinetic interactions of two simultaneously administered drugs.

Eq. (5) comprises a term (log k_{IAM}) that cannot be obtained from computational chemistry. Hence, to use it, one needs some (however minute) amounts of the existing substance. There is a hydrophobicity parameter that can be calculated from the structural formula, i.e., *CLOGP* [38–40]. For 38 drugs for which both log k_{IAM} and *CLOGP* were available, the correlation between them was $R = 0.850$. Replacing log k_{IAM} in Eq. (5) by *CLOGP* decreases the correlation, however, the resulting regression equation remains significant and, hence, informative. Most probably, the predictive power of *CLOGP*

Table 2
Logarithms of chromatographic retention factors determined on an α_1-acid glycoprotein HPLC column, log k_{AGP}, and on an immobilized artificial membrane column, log k_{IAM}, and structural parameters of a series of basic drugs [32]

Drug name	log k_{AGP}	log k_{IAM}	*CLOGP*[a]	N_{ch}	S_T
Antagonists of H_1 histamine receptor					
Antazoline	1.154	1.043	4.25	−0.285	25.23
Chlorpheniramine	1.202	1.055	2.73	−0.260	30.92
Chloropyramine	1.431	1.330	3.56	−0.268	31.11
Cinnarizine	2.148	2.250	6.14	−0.248	32.18
Dimethindene	1.382	1.194	3.42	−0.267	29.76
Diphenhydramine	1.140	1.006	3.36	−0.266	32.78
Isothipendyl	1.580	1.210	3.93	−0.260	20.41
Ketotifen	1.459	1.168	3.56	−0.245	25.54
Mepyramine	1.113	0.935		−0.272	32.81
Pheniramine	0.926	0.602	2.02	−0.260	27.37
Pizotifen	1.898	1.588		−0.247	29.13
Promethazine	1.833	1.508	4.65	−0.257	20.73
Tripelennamine	1.066	0.887	2.85	−0.264	30.37
Triprolidine	1.185	1.084	3.47	−0.240	24.02
Tymazoline	1.306	1.204		−0.287	17.07
Antagonists of H_2 histamine receptor					
Cimetidine	0.482	−0.271	0.21	−0.195	18.11
Famotidine	0.731	−0.271	−0.57	−0.161	27.44
Metiamide	0.517	−0.301	0.38	−0.193	19.19
Nizatidine	0.460	−0.368		−0.275	32.01
Ranitidine	0.600	−0.016	0.27	−0.262	31.86
Roxatidine	0.773	0.359	2.66	−0.279	28.99
Antagonists of β-adrenoceptors					
Acebutolol	0.676	0.602	1.61	−0.300	49.35
Alprenolol	1.490	0.918	2.59	−0.299	25.99
Atenolol	0.499	−0.146	−0.11	−0.298	20.36
Betaxolol	0.838	0.994	2.17	−0.300	27.00
Bisoprolol	0.694	0.646	1.69	−0.297	45.07
Bopindolol	1.940	0.456	4.86	−0.301	38.39
Bupranolol	0.981	0.269		−0.291	21.76
Carteolol	0.706	−0.146	1.17	−0.289	24.88
Celiprolol	0.700	0.723	1.66	−0.304	37.28
Cicloprolol	0.735	1.012		−0.298	42.28
Dilevalol	1.106	1.272	2.18	−0.295	27.49
Esmolol	0.649	0.646	1.53	−0.299	30.30
Metoprolol	0.564	0.434	1.20	−0.301	22.66
Nadolol	0.606	0.269		−0.292	29.90
Nifenalol	0.639	0.269	1.16	−0.300	12.19
Oxprenolol	1.210	0.586	1.62	−0.299	28.60
Pindolol	0.870	0.586	1.65	−0.301	27.79
Practolol	0.509	−0.067	0.78	−0.301	22.74
Propranolol	1.612	1.340	2.75	−0.300	28.77
Sotalol	0.516	−0.146	0.23	−0.178	19.40
Timolol	0.696	0.385	1.63	−0.290	15.60
Agonists and antagonists of α-adrenoceptors					
Cirazoline	1.082	0.940	3.27	−0.288	16.78
Clonidine	0.847	0.410		−0.278	12.32
Doxazosin	1.798	1.983	3.77	−0.307	30.64
Moxonidine	0.528	−0.067		−0.286	13.35
Naphazoline	1.092	0.895	3.83	−0.295	17.61
Phentolamine	1.264	1.340	3.68	−0.289	24.30
Prazosin	1.390	1.594	2.16	−0.308	31.47
Tiamenidine	0.808	0.434		−0.284	9.96
Tramazoline	1.315	1.123	2.49	−0.285	21.22
UK-14,304	0.831	0.269		−0.276	15.74

[a] Logarithm of *n*-octanol–water partition coefficient calculated by the fragmental method, taken from Craig [38].
[b] Electron excess charge on aliphatic nitrogen.
[c] Area (in Å) of the size/shape triangle (see Fig. 4).

could increase if a correction due to ionization at the actual pH was introduced. The problem in individual cases is, however, to acquire the required pK_a values.

The QSRR equation derived here and the reported [26–30] qualitative characteristics of the mode of binding of xenobiotics by AGP allow for an indirect identification of structural features of the binding site of basic drugs (Fig. 5). The site can be modeled by an open conical pocket. Its wall (internal surface) contains lipophilic regions at the base of the cone. There is an anionic region close to the spike of the cone. Protonated aliphatic nitrogen guides drug molecules towards the anionic region. Hydrophobic hydrocarbon fragments of the interacting drugs provide anchoring in the lipophilic region(s) of the binding site. There is a steric restriction for the molecule to plunge into the binding site. Asymmetric charge distribution accounts for the observed enantioselectivity of binding to AGP. Similarly, asymmetric distribution of charge (positive) in one of the two benzodiazepine binding sites on HSA (Fig. 3) accounted for the observed stereoselectivity of binding.

Norinder and Hermansson [41] attempted to relate the structure of a series of *N*-aminoalkyl-succinimides to their enantioselectivity factors, α, observed on an AGP column. In order to derive a model to describe the behavior of 33 solutes, 50 structural descriptors were subjected to a chemometric data processing procedure, called principal component analysis (PCA). The four main abstract factors extracted by PCA were then used to calculate a regression equation to predict α values. The correlation between the experimental and calculated data was characterized by $R^2 = 0.86$. To arrive at this correlation, the authors had to introduce ten arbitrary indicator variables (including their squares, the meaning of which is especially obscure). The description of enantioselectivity in terms of abstract principal components makes the interpretation in physical terms barely possible. In addition, the use of this approach for the prediction of α for a given analyte would require tedious structural assignments and recalculations.

4. Keratin column

It is well known that hydrophobicity (lipophilicity) of drugs strongly affects their skin permeation properties. Hydrophobicity determines the affinity of drugs for adipose (fat) cells in the subcutaneous layer of the skin and for biomembranes of other

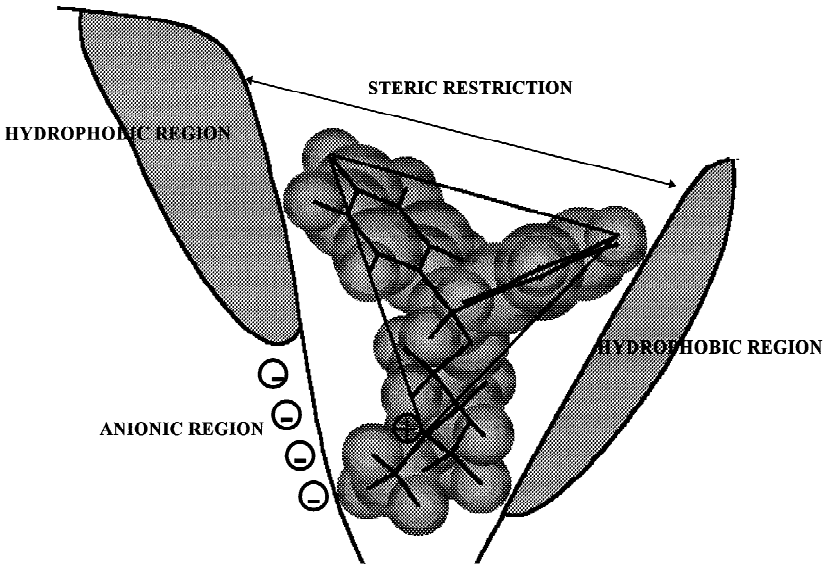

Fig. 5. Mode of binding of basic drugs by α_1-acid glycoprotein. See text for discussion.

cells. However, to reach the fat tissue, the drug must first cross the epidermis. The outermost layers of epidermis comprises large amounts of keratin. Hence, to model the skin permeation process, both the hydrophobicity of drugs and their possible interactions with keratin should be taken into account.

HPLC columns comprising keratin were prepared [42,43] by physical immobilization of the protein on a silica support and by slurry packing of standard 12.5 cm×4 mm I.D. columns.

A series of test solutes were chromatographed using phosphate buffer as an eluent. The retention parameters, log k_{KER}, are shown in Table 3, along with the hydrophobicity parameter determined [37] on an IAM column, log k_{IAM}, and the logarithms of human skin permeation coefficient, log K_p, taken from the literature [44–47].

QSARs describing log K_p in terms of a hydrophobicity parameter, log k_{IAM}, proves the importance of the hydrophobicity of drugs for their permeation through the skin:

$$\log K_p = 1.458(\pm 0.138) \log k_{IAM} - 6.420(\pm 0.139) \quad (6)$$

$n = 17; R = 0.899; s = 0.47; p \leq 10^{-4}$

Adding the term log k_{KER} to Eq. (6) improves the predictiveness of the resulting two-parameter QSAR equation:

$$\log K_p = 1.920(\pm 0.242) \log k_{IAM} - 1.039(\pm 0.413) \log k_{KER} - 6.558(\pm 0.130) \quad (7)$$

$n = 17; R = 0.932; s = 0.40; p \leq 10^{-4}$

The plot of the observed human skin permeation data, log K_p, against the ones calculated by Eq. (7) is given in Fig. 6. The prediction of skin permeability of test agents is good and the regression equation, Eq. (7), can be of practical value for rational drug design.

Eq. (7) is not only significant statistically but it also makes good physical sense. It shows that skin permeability increases with the lipophilicity of the agents, but decreases with their affinity to keratin. In other words, keratolytic properties of phenols and other acidic test compounds oppose their lipophilic properties as regards skin permeation. It should be noted at the same time that the coefficient at log k_{IAM}

Table 3
Logarithms of retention factors determined on the keratin column, log k_{KER} [42], on the collagen column, log k_{COLL} [48] and on the immobilized artificial membrane column, log k_{IAM} [37] and logarithms of the human skin permeation coefficient, log K_p [44–47] for a series of phenols and other simple organic compounds

No.	Analyte	log k_{KER}	log k_{COLL}	log k_{IAM}	log K_p
1	2-Cresole	−0.178	−0.74	0.363	−5.36
2	2-Naphthol	0.879	−0.15	1.254	−5.11
3	3-Cresole	−0.223	−0.74	0.363	−5.37
4	3-Nitrophenol	0.241	−0.70	0.598	−5.81
5	4-Bromophenol	0.338	−0.44	0.995	−5.00
6	4-Chlorophenol	0.273	−0.92	0.728	−5.00
7	4-Cresole	−0.082	−0.74	0.418	−5.31
8	4-Ethylphenol	−0.249	−0.70	0.761	−5.01
9	4-Nitrophenol	0.189	−0.70	0.595	−5.81
10	Baclofen	−0.334	−0.92	−0.725	−6.77
11	Chlorocresole	0.678	−0.66	1.183	−4.82
12	Methylhydroxybenzoate	0.044	−0.74	0.520	−5.60
13	Phenol	−0.273	−0.88	0.366	−5.64
14	Phenylalanine	−0.198	−1.33	−0.646	−8.08
15	Resorcinol	−0.382	−0.95	−0.141	−7.18
16	Salicylic acid	−0.058	0.06	−0.575	−7.82
17	Thymol	0.521	−0.38	1.342	−4.83

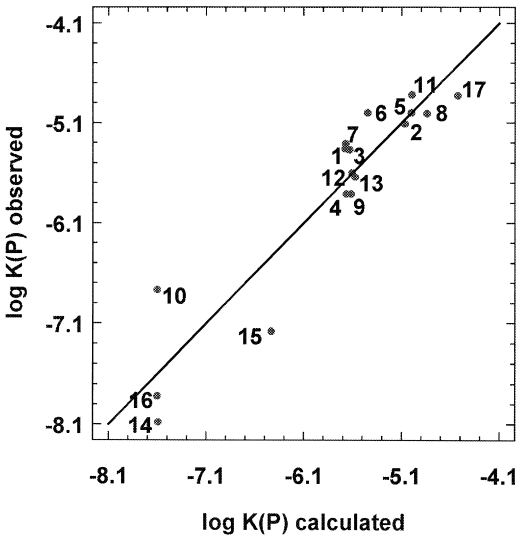

Fig. 6. Plot of logarithms of human skin permeability by agents listed in Table 3 observed experimentally against the corresponding data calculated theoretically using Eq. (7).

in Eq. (7) is nearly two times larger than the coefficient at the log k_{KER} term. As the net effect, the phenol derivatives should be absorbed from skin, which is experimentally observed.

5. Collagen columns

While developing the idea of applying affinity chromatographic retention parameters to model skin permeation, we turned our attention to the presence of collagen fibres in upper skin layers, i.e. epidermis and dermis [48]. Consequently, the new stationary phases for HPLC were synthesized by covalently binding collagen to aminopropylsilica and diol–silica materials. The collagen phases were demonstrated to exhibit different mechanism of retention from that observed on either keratin or IAM columns. Polar, hydrophilic properties of collagen manifested themselves clearly in QSRRs.

For the series of thirteen test analytes given in Table 4, a significant QSRR equation describes retention in terms of total dipole moment, μ, and another structural descriptor, *MaxMin*. The latter descriptor is defined as the largest difference (in electrons) between the maximum and the minimum atomic excess charges in the molecule:

$$\log k_{COLL} = -0.043(\pm 0.009)\,\mu + 0.629(\pm 0.166)\,MaxMin - 0.982(\pm 0.101) \quad (8)$$

$n = 13$; $R = 0.860$; $s = 0.155$; $p \leq 0.002$

Table 4
Logarithms of retention factors determined on the collagen column, log k_{COLL}, and structural parameters of analytes from molecular modeling: μ, total dipole moment, and *MaxMin*, the largest difference between the maximum and minimum atomic excess charge in the molecule [48]

No.	Analyte	μ [D]	*MaxMin* [e]	log k_{COLL}
1	1,2,3-Tris(methylethyl) benzene	0.0002	0.336	−0.88
2	1,4-Dinitrobenzene	0	0.907	−0.57
3	3-(Trifluoromethyl)phenol	4.393	0.710	−0.57
4	4-Chlorophenol	2.184	0.468	−0.92
5	4-Nitrobenzoic acid	11.772	0.914	−0.81
6	Anisole	1.560	0.360	−0.81
7	Benzene	0	0.260	−0.78
8	Benzonitrile	11.122	0.280	−1.48
9	Caffeine	13.749	0.759	−1.06
10	Chlorobenzene	1.708	1.093	−0.40
11	Indazole	2.390	0.479	−0.63
12	Phenol	1.520	0.470	−0.88
13	Toluene	0.069	0.309	−0.52

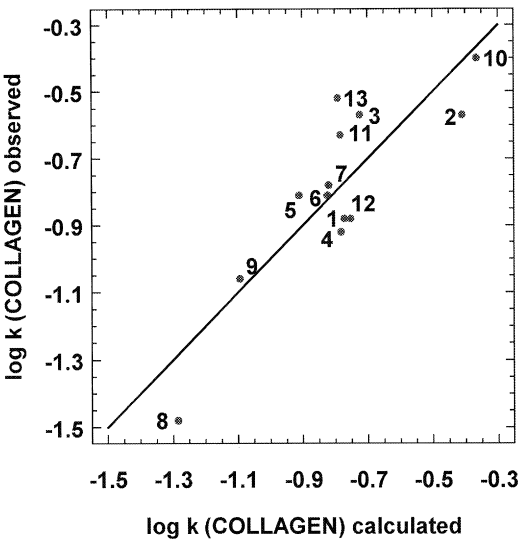

Fig. 7. Plot of logarithms of the capacity factor, determined for compounds listed in Table 4 on the collagen column, against the corresponding data calculated theoretically using Eq. (8).

The predictive potency of Eq. (8) is illustrated in Fig. 7.

The *MaxMin* parameter in Eq. (8) can be treated as a measure of local dipole, whereas μ is the total dipole moment. Both parameters undoubtedly reflect differences in polar properties within the set of test analytes. None of the molecular size-related (''bulkiness'') structural descriptors tested appeared significant in QSRR analysis. One can thus conclude that the normal-phase retention mechanism prevails on the collagen phase.

To check the performance of the collagen column in modeling human skin permeation by xenobiotics, the biological data from Table 3 were considered. It appeared that the log k_{COLL} parameter did not improve prediction of human skin permeation provided by the combination of log k_{KER} and log k_{IAM} (Eq. (7)).

The agents listed in Table 3 (mostly phenols) have their skin permeation determined by lipophilicity (positive effect) and by affinity to keratin (negative effect). Interactions with collagen are certainly of lesser importance. Hence, they are difficult to demonstrate, bearing in mind the naturally limited precision of skin permeability data. If a set of skin permeation data for those xenobiotics that strongly interact with collagen is available, the inputs to modeling skin permeation due to the collagen phase could be proved more clearly.

6. Melanin column

Natural melanins (rheomelanins containing sulphur and eumelanins that do not contain sulphur) are biopolymers composed mainly of indole-5,6-quinone units with several dopachrome and 5,6-dihydroxyindole carboxylic moieties. Synthetic melanins are prepared from L-dopa. They contain more carboxylic groups than natural melanins. No significant differences in ligand affinity were reported between natural melanins and synthetic polymers [49].

High affinity for melanin correlates with ocular toxicity, ototoxicity, pigment disturbances of the skin and hair, carcinogenicity and extrapyramidal disorders caused by drugs [50–52]. Hence, the means to measure and predict binding of drugs by melanin would be important. Having the above in mind, the silica-based stationary phases for HPLC were prepared with physically [53] and chemically [54] immobilized synthetic melanin.

Retention parameters, log k_{MEL}, determined on a column packed with chemically immobilized melanin–silica stationary phase, are given in Table 5 for a series of psychotropic drugs (mostly phenothiazine neuroleptics) [55]. The mobile phase was 0.1 *M* sodium phosphate buffer–propanol 95:5 (v/v). For seven drugs of the series, the binding to synthetic melanin was determined by an ultrafiltration method. The drug–melanin interaction parameters from affinity HPLC and those determined by a standard ultrafiltration approach showed significant correlation ($p=0.05$). Certainly, the chromatographically determined, highly reproducible, retention factor is a more reliable melanin-binding parameter than that obtained by the slow-equilibrium ultrafiltration method. The poor Scatchard plots observed with the ultrafiltration method are probably due to complication of the structurally specific binding by nonspecific adsorption on the surface of melanin particles and to nonhomogeneity of the synthetic melanin preparations.

By applying affinity HPLC, the melanin-binding

Table 5
Logarithms of retention factors determined on the melanin column, log k_{MEL} [55] and on the immobilized artificial membrane column, log k_{IAM} [53] and the energy of lowest unoccupied molecular orbital, E_{LUMO} [55], for a series of neuroleptic drugs and inactive phenothiazine derivatives

No.	Phenothiazine analyte	log k_{MEL}	log k_{IAM}	E_{LUMO} (eV)
1	Promethazine	1.021	1.325	−0.0494
2	Promazine	1.130	1.353	−0.2026
3	Fluphenazine	1.290	1.654	−0.8929
4	Chlorpromazine	1.267	1.624	−0.4826
5	Thioridazine	1.312	2.042	−0.4453
6	Trimeprazine	1.021	1.319	−0.2081
7	Trifluoperazine	1.243	2.066	−0.8731
8	Trifluopromazine	1.176	1.674	−0.8813
9	Prochlorperazine	1.279	2.050	−0.4945
10	Propiomazine	1.190	1.412	−0.2988
11	Perphenazine	1.290	1.612	−0.5068
12	Ethopromazine	0.929	1.242	−0.0510
13	Clomipramine	1.096	1.577	−0.2513
14	Imipramine	0.903	1.267	−0.1456
15	Acetopromazine	1.113	1.270	−0.4420

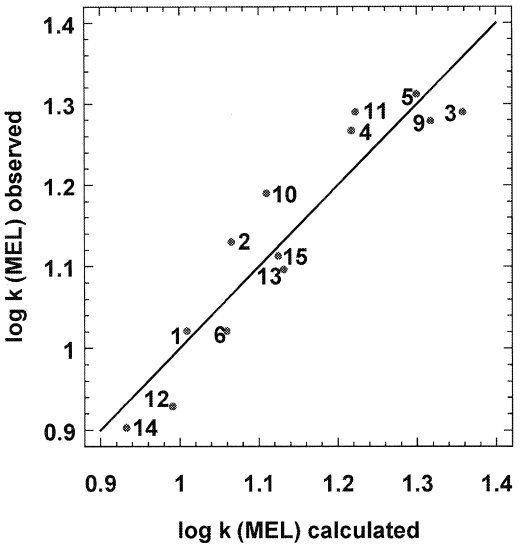

Fig. 8. Plot of logarithms of the capacity factor, determined for compounds listed in Table 5 on the melanin column, against the corresponding data calculated theoretically using Eq. (9).

measures could readily be obtained for series of analytes that are long enough, which are required to derive QSRRs.

To derive QSRR equations, several structural parameters of test analyte drugs were considered, obtained either empirically or from molecular modeling. The resulting regression equation is:

$$\log k_{MEL} = -0.2247(\pm 0.0730)\log k_{IAM} - 0.3256(\pm 0.0760)E_{LUMO} + 0.696(\pm 0.010) \quad (9)$$

$n = 13$; $R = 0.933$; $s = 0.056$; $p \leq 0.0001$

where log k_{IAM} is a drug hydrophobicity parameter determined chromatographically on an immobilized artificial membrane column and E_{LUMO} is the energy of the lowest unoccupied molecular orbital from molecular modeling. Two drugs from Table 5 (trifluoperazine and trifluopromazine) did not fit Eq. (9) and were excluded from regression. The reason may be the inadequacy of the applied quantum chemical software (MOPAC package within Insight II, Biosym Technologies, San Diego, CA, USA) to account for the structural specificity of fluorinated compounds.

Eq. (9) has a good predictive potency (Fig. 8) and can be used to estimate the relative melanin-binding properties of new phenothiazines and dibenzazepines (and perhaps other structurally similar xenobiotics). According to Eq. (9), retention by the melanin stationary phase increases with the lipophilicity of drugs. The presence of E_{LUMO} can be interpreted as a proof of significance of the charge-transfer interactions for the formation of the drug–melanin complex. Such interactions for single individual drugs have been postulated by other authors [56,57], but have not been proved. The probable interacting functionalities on melanin could be the carboxylic and/or quinone moieties. Eq. (9) provides a quantitative proof of the involvement of the charge-transfer intermolecular interactions, along with hydrophobic interactions, in the formation of complexes between melanin and both phenothiazine and dibenzazepine drugs.

7. Amylose tris(3,5-dimethylphenylcarbamate) column

Booth and Wainer [58] applied chemometric analysis to retention factors of a series of 28 chiral α-alkyl arylcarboxylic acids determined on a chiral

stationary phase based upon amylose tris(3,5-dimethylphenylcarbamate) (AD). The retention data were correlated to a series of structural descriptors. The QSERR equations derived incorporated the hydrogen bond ability and aromaticity of test analytes. For the first-eluting enantiomer the multiple regression equation was:

$$\ln k_1 = -2.499 + 1.369(\pm 0.177)X + 0.791(\pm 0.121)Y + 0.415(\pm 0.094)Z \quad (10)$$

$$n = 26;\ R = 0.947;\ p \leq 0.0001$$

The respective QSRR for the second-eluting isomer was:

$$\ln k_2 = -2.659 + 1.498(\pm 0.151)X + 0.896(\pm 0.103)Y + 0.439(\pm 0.080)Z \quad (11)$$

$$n = 26;\ R = 0.967;\ p \leq 0.0001$$

In Eqs. (10) and (11), X and Y are the numbers of hydrogen bond donors and acceptors, respectively, and Z is the degree of aromaticity in the molecule.

In molecular modeling studies, Booth and Wainer [58] identified a site within the helical ravine of an AD model at which enantioselective discrimination of analytes occurs. Benoxaprofen was docked in this ravine (the drug was chosen as the test molecule as it demonstrated the highest retention and enantioselectivity of the series). When benoxaprofen is docked in the ravine, there is a potential for three simultaneous hydrogen-bonding interactions (Fig. 9). Two of those interactions can occur between the carbonyl oxygen and acid hydroxyl proton on the acid moiety of benoxaprofen and the amide proton and the ether oxygen on the AD stationary phase. A third hydrogen bond can be formed between an amide proton on AD and the oxygen and/or nitrogen atom in the five-membered oxazole ring.

Booth and Wainer [58] argue that, even though enantiomers form identical hydrogen-bonding interactions, and presumably the same hydrophobic interactions as well, the diastereomeric benoxaprofen–AD complexes differ in their stabilities, leading to chiral discrimination. The difference arises from the internal energies of the two enantiomer conformations. The bonding conformation of (*R*)-benoxaprofen is approximately 250 cal/mol higher in energy than that of (*S*)-benoxaprofen.

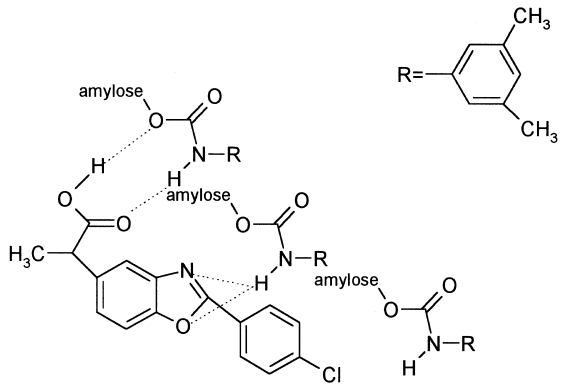

Fig. 9. Mechanism of binding of benoxaprofen by amylose tris(3,5-dimethylphenylcarbamate) showing the hydrogen-bonding sites proposed by Booth and Wainer [58].

The conclusion drawn by Booth and Wainer [58] is that, unlike the standard ''three-point interaction'' model of chiral recognition, enantioselectivity on AD is due to a ''conformationally driven'' chiral recognition process.

In further studies on the molecular mechanism of enantioselective separation on the AD chiral stationary phase, Booth and Wainer [59] derived QSERR equations for a drug, mexiletine, and a series of eleven structurally related compounds. These equations described retention factors of the first- and the second-eluting enantiomers in terms of fragmental hydrophobicities of selected substituents and analyte polarity descriptors (total aromatic electron excess charge, substructure dipole). By application of QSERR and the enthalpy–entropy compensation analysis, two distinctive retention mechanisms of mexiletine-related compounds on the AD stationary phase were identified. These mechanisms are based on either the presence or absence of secondary hydrogen-bonding groups.

The most recent study by Booth et al. [60], aimed at the prediction of chiral chromatographic separation of 29 aromatic acids and amides on three amylose-based stationary phases, is very interesting. The chemometric tools applied by the authors were multiple regression analysis (MRA) and neural networks analysis (NNA).

Structural descriptors of analytes produced by

molecular modeling, which appeared to be the most suitable for MRA and NNA, were: molecular electrostatic potential (MEP), molecular lipophilic potential (MLP), dipole moment (DIP) and energy of the lowest unoccupied molecular orbital (LUMO). The LUMO and MLP parameters affected retention most strongly. The LUMO suggested the charge transfer interactions to occur between the analytes and the AD phases studied. The MLP descriptor, according to the authors [60], incorporates a combination of lipophilicity with steric and geometric factors.

The MRA was able to provide information regarding the fundamental mechanistic interactions incorporated in the retention on AD phases. However, as regards retention prediction based on structural descriptors of analytes, the NNA provided better models.

8. Other immobilized biomacromolecule columns

Chemometric analysis of enantioselective retention data was first reported by Wolf et al. [61]. These authors applied multiple regression analysis to relate enantioselective resolutions on cellulose triacetate and cellulose tribenzonate columns to structural descriptors of analytes [62–65]. Apart from analytical applications, i.e., prediction of separation of optical isomers of individual chemical families, the studies shed some light on the supramolecular structure of cellulose.

Computational studies of enantioselective separations on the cellulose triacetate chiral stationary phase were also reported by Roussel and Popescu [66] and Isaksson et al. [67].

In a recent QSRR study, the retention of twenty nonsteroidal antiinflammatory drugs (NSAIDs) on immobilized zein (a wheat protein) was considered [68]. The interactions of NSAIDs with the protein were related to their structural descriptors from molecular modeling by means of advanced multivariate data processing methods: PCA and cluster analysis. It was established that the polarity and steric descriptors of NSAIDs exerted the largest influence on the drugs' interactions with zein. No separation of enantiomers of NSAIDs tested was observed under the HPLC conditions applied, although marked differences in retention (and binding to zein) were noted among the drug analytes studied.

9. Concluding remarks

QSRR equations (Eqs. (1)–(5)) account, in strict statistical terms, for the properties qualitatively ascribed to the drug binding sites on HSA and AGP. Of course, it would be interesting to relate these working models to the structures of the drug–HSA and drug–AGP crystals once they are resolved. It must be stressed, however, that while crystallographic analysis helps to visualize supposed active sites on biomacromolecules, the pictorial presentation is of limited use in predicting the binding of agents of a given chemical structure. Reliable predictions of activity and the determination of the required structural properties for the design of new drugs are facilitated by good quantitative structure–pharmacological activity relationships. To derive such relationships, one needs larger sets of numerically expressed biological (biorelevant) data. Such are the retention data determined by means of the HPLC systems containing biomacromolecules.

Biological activity parameters are normally a net result of often opposing effects. One can model these individual effects chromatographically and then evaluate their mutual inputs to the biologically measured quantity by chemometric procedures. In effect, rational explanations of the observed phenomena can result, as well as the means to predict bioactivity for the biologically untested structures based on the chromatographic data and calculations. That way, human skin permeation of agents can be evaluated based on their hydrophobicity and retention on a keratin column (and, perhaps, for some agents, additionally on a collagen column). Large sets of drug–biomacromolecule interaction data readily produced by affinity HPLC can serve to interpret the mechanism of those interactions at the molecular level. Next, it should be possible to predict the potency of a given drug or drug candidate to take part in vital intermolecular interactions in a living system.

The quantities produced by affinity HPLC for individual drugs need not be identical to the drug–biomacromolecule interaction data from standard slow equilibrium experiments. Affinity HPLC is unable to produce absolute values of binding. However, assuming linear free-energy relationships (LFERs), one can chromatographically compare the ability of individual members of a series of analytes to form complexes with a given biomacromolecule, which is an active component of a defined separation system.

QSRRs or QSERRs provide an insight into the mechanism of separation (enantioseparation) on immobilized biomacromolecules at a molecular or even a submolecular level. Thus, selection of chromatographic separation systems for solving individual analytical problems can be guided rationally. Also, based on QSRRs, a search for stationary phases of specific requested properties can be facilitated.

The combination of affinity chromatography and chemometrics appears to be a promising strategy in biologically oriented research. It offers increased speed and efficiency in establishing quantitative relationships between the chemical structure of xenobiotics and their ability to participate in intermolecular interactions with the components of a living system. By that approach, there is also a chance of decreasing the costs of a search for new drugs and the use of laboratory animals. The perspectives now are especially attractive because of the availability of isolated pharmacological receptors obtained by modern biotechnology.

References

[1] R. Kaliszan, Quantitative Structure–Chromatographic Retention Relationships, Wiley, New York, 1987.
[2] R. Kaliszan, Chemometr. Intell. Lab. Syst. Lab. Inf. Manage. 24 (1994) 89.
[3] N.D. Danielson, R.W. Siergiej, Biotechnol. Bioeng. 23 (1981) 1913.
[4] S. Kamada, M. Maeda, A. Tsui, Y. Umezawa, T. Kurahashi, J. Chromatogr. 239 (1982) 773.
[5] S.C. Crowley, R.R. Walters, J. Chromatogr. 266 (1983) 157.
[6] S. Allenmark, B. Bomgren, H. Borén, J. Chromatogr. 264 (1983) 63.
[7] J. Hermansson, J. Chromatogr. 269 (1983) 71.
[8] E. Domenici, C. Bertucci, P. Salvadori, G. Félix, I. Cahagne, S. Motellier, I.W. Wainer, Chromatographia 29 (1990) 170.
[9] T. Miwa, M. Ichikawa, M. Tsuno, T. Hattori, T. Miyakawa, M. Kano, Y. Miyake, Chem. Pharm. Bull. 35 (1987) 682.
[10] N. Mano, Y. Oda, N. Asakawa, Y. Yoshida, T. Sato, T. Miwa, J. Chromatogr. 623 (1992) 221.
[11] J. Haginaka, T. Murashima, C. Seyama, J. Chromatogr. A 677 (1994) 229.
[12] J. Haginaka, Y. Miyano, Y. Saizen, C. Seyama, T. Murashima, J. Chromatogr. A 708 (1995) 161.
[13] B. Sebille, R. Zini, C.-V. Madjar, N. Thuaud, J.-P. Tillement, J. Chromatogr. 531 (1990) 51.
[14] L. Soltes, B. Sebille, Chirality 9 (1997) 373.
[15] J. Oravcová, B. Böhs, W. Lindner, J. Chromatogr. A 677 (1996) 1.
[16] J. Gao, M. Mammen, G.W. Whitesides, Science 272 (1996) 535.
[17] D.S. Hage, S.A. Tweed, J. Chromatogr. B 699 (1997) 499.
[18] R. Kaliszan, I.W. Wainer, in K. Jinno (Editor), Chromatographic Separations Based on Molecular Recognition, Wiley–VCH, New York, 1997, p. 273.
[19] R. Kaliszan, Structure and Retention in Chromatography. A Chemometric Approach, Harwood Academic Publishers, Amsterdam, 1997.
[20] I.W. Wainer, J. Chromatogr. A 666 (1994) 221.
[21] A.-F. Aubry, A. McGann, LC·GC Int. 7 (1994) 389.
[22] T.A.G. Noctor, C.D. Pham, R. Kaliszan, I.W. Wainer, Mol. Pharmacol. 42 (1992) 506.
[23] R. Kaliszan, T.A.G. Noctor, I.W. Wainer, Mol. Pharmacol. 42 (1992) 512.
[24] T. Alebić-Kolbah, F. Kajfez, S. Rendić, V. Sunjić, A. Konowal, G. Snatzke, Biochem. Pharmacol. 28 (1979) 2457.
[25] D.S. Ashton, C.R. Beddell, G.S. Cockerill, K. Gohil, C. Gowrie, J.E. Robinson, M.J. Slater, K. Valko, J. Chromatogr. B 677 (1996) 194.
[26] J.M.H. Kremer, J. Wilting, L.H.M. Janssen, Pharmacol. Rev. 40 (1988) 1.
[27] J. Schley, J. Pharm. Pharmacol. 39 (1987) 132.
[28] L. Soltes, B. Sebille, P. Szalay, J. Pharm. Biomed. Anal. 12 (1994) 1295.
[29] H. Glaser, J. Kriegelstein, Naunyn-Schmiedeberg's Arch. Pharmacol. 265 (1970) 321.
[30] D.L. Goolkasian, R.L. Slaughter, D.J. Edwards, D. Lalka, Eur. J. Clin. Pharmacol. 25 (1983) 413.
[31] A. Nasal, A. Radwańska, K. Ośmialowski, A. Buciński, R. Kaliszan, G.E. Barker, P. Sun, R.A. Hartwick, Biomed. Chromatogr. 8 (1994) 125.
[32] R. Kaliszan, A. Nasal, M. Turowski, Biomed. Chromatogr. 9 (1995) 211.
[33] R. Kaliszan, A. Nasal, M. Turowski, J. Chromatogr. A 722 (1996) 25.
[34] H. Thurnhofer, J. Schnabel, M. Betz, G. Lipka, C. Pidgeon, H. Hauser, Biochim. Biophys. Acta 1064 (1991) 275.
[35] C. Pidgeon, C. Marcus, F. Alvarez, in T.O. Baldwin, J.W. Kelly (Editors), Applications of Enzyme Biotechnology, Plenum Press, New York, 1992, p. 201.
[36] R. Kaliszan, A. Kaliszan, I.W. Wainer, J. Pharm. Biomed. Anal. 11 (1993) 505.
[37] A. Nasal, M. Sznitowska, A. Buciński, R. Kaliszan, J. Chromatogr. A 692 (1995) 83.

[38] P.N. Craig, in C. Hansch, P.G. Sammes, J.B. Taylor (Editors), Comprehensive Medicinal Chemistry, Vol. 6, Pergamon Press, Oxford, 1990.
[39] R.F. Rekker, The Hydrophobic Fragmental Constant, Elsevier, Amsterdam, 1977.
[40] C. Hansch, A. Leo, Substituent Constants for Correlation Analysis in Chemistry and Biology, Wiley, New York, 1979.
[41] U. Norinder, J. Hermansson, Chirality 3 (1991) 422.
[42] M. Turowski, R. Kaliszan, J. Pharm. Biomed. Anal. 15 (1997) 1325.
[43] R. Kaliszan, M. Turowski, Polish Patent No. P313926.
[44] M.S. Roberts, R.A. Anderson, J. Swabrick, J. Pharm. Pharmacol. 29 (1977) 677.
[45] T. Kurihara-Bergstrom, K. Knutson, L.J. De Noble, C.Y. Goates, Pharm. Res. 7 (1990) 762.
[46] A. Ruland, J. Kreuter, Int. J. Pharm. 72 (1991) 149.
[47] G.C. Mazzenga, B. Berner, F. Jordan, J. Control. Release 20 (1992) 163.
[48] M. Turowski, R. Kaliszan, Biomed. Chromatogr., 12 (1998), in press.
[49] M. Salazar, T. Sokoloski, P.N. Patil, Fed. Proc. 37 (1978) 2403.
[50] A.M. Potts, Invest. Ophthalmol. 3 (1964) 405.
[51] B. Larsson, H. Tjälve, Biochem. Pharmacol. 28 (1979) 1181.
[52] B.S. Larsson, Pig. Cell Res. 6 (1993) 127.
[53] R. Kaliszan, A. Kaliszan, I.W. Wainer, J. Chromatogr. 615 (1993) 281.
[54] H. Ibrahim, A.-F. Aubry, Anal. Biochem. 229 (1995) 272.
[55] A. Radwańska, T. Frąckowiak, H. Ibrahim, A.-F. Aubry, R. Kaliszan, Biomed. Chromatogr. 9 (1995) 233.
[56] H. Tjälve, M. Nilsson, B. Larsson, Biochem. Pharmacol. 30 (1981) 1845.
[57] K.B. Stępień, T. Wilczok, Biochem. Pharmacol. 31 (1982) 3359.
[58] T.D. Booth, I.W. Wainer, J. Chromatogr. A 737 (1996) 157.
[59] T.D. Booth, I.W. Wainer, J. Chromatogr. A 741 (1996) 205.
[60] T.D. Booth, K. Azzaoui, I.W. Wainer, Anal. Chem. 69 (1997) 3879.
[61] R.M. Wolf, E. Francotte, D. Lohman, J. Chem. Soc., Perkin Trans. 2 1988 (1988) 893.
[62] E. Francotte, R.M. Wolf, Chirality 2 (1990) 16.
[63] E. Francotte, D. Lohman, Helv. Chim. Acta 70 (1987) 1569.
[64] E. Francotte, R.M. Wolf, Chirality 3 (1991) 43.
[65] E. Francotte, R.M. Wolf, D. Lohman, J. Chromatogr. 347 (1985) 25.
[66] C. Roussel, C. Popescu, Chirality 6 (1994) 251.
[67] R. Isaksson, H. Wennerstrom, O. Wennerstrom, Tetrahedron 44 (1988) 1647.
[68] E. Forgacs, A. Kosa, G. Csiktusnadi Kiss, R. Kaliszan, P. Haber, A. Nasal, J. Liq. Chromatogr., (1998), in press.